

Effect of the spectral broadening of the first Stokes component on the efficiency of a two-stage Raman converter

O.N. Egorova, A.S. Kurkov, O.I. Medvedkov, V.M. Paramonov, E.M. Dianov

Abstract. A two-stage Raman fibre converter (1.089/1.273/1.533 μm) based on a P₂O₅-doped silica fibre is fabricated and studied. The spectral broadening of the first Stokes component is investigated. The Raman converter is simulated numerically. By using the experimental data, the method of Raman converter simulation is improved by taking into account the additional power loss of the first Stokes component. The results of calculations by the improved method are in good agreement with the experiment. It is shown that the additional power loss of the first Stokes component results in a change in the region of the optimal resonator length from 300–600 m to 600–800 m.

Keywords: Raman fibre converter, phosphosilicate fibre.

1. Introduction

The development of high-power pump sources made it possible to create fibre lasers or converters based on multistage stimulated Raman scattering (SRS) and emitting virtually over the entire transparency range of silica fibres [1, 2]. The comparatively high power and a broad tuning range provided applications of Raman converters for pumping fibre amplifiers [3, 4], in medicine [5], etc.

The efficiency of a Raman converter depends on several factors such as the fibre length, pump power, parameters of the fibre and fibre Bragg gratings (FBGs). The optimisation of a Raman converter usually involves an appropriate selection of the fibre length and FBG reflectivity, which can be performed with the help of the theoretical model proposed in [6]. It is this model that was used to optimise Raman converters in [7–9].

The converter model [6–9] assumes that the pump and Stokes radiations are quasi-monochromatic. However, a finite spectral width of the Stokes components in real Raman converters can lead to the discrepancy between calculations and experimental results, for example, due to the additional power losses in the resonator. These losses appear because the width of a Stokes component is larger

than the reflection spectrum of the corresponding FBG. The escape of a part of the power of the intermediate Stokes component from the resonator was observed in [10, 11].

In this paper, we improved the Raman converter model by introducing the effective reflectivity of the 1.273-μm FBGs in the first stage, which takes into account the escape of a part of the first Stokes component power from the resonator. This gave good agreement with the experimental results obtained for a 1.533-μm Raman converter. The converter was optimised over the resonator length and the reflectivity of the output grating for the 4.4-W pump power, and the optimal region of values of these parameters for this Raman converter was found.

2. Description of the model

Figure 1 shows the scheme of the Raman fibre converter. The two-stage frequency conversion (1.089/1.273/1.533 μm) is performed in a P₂O₅-doped silica fibre. The resonator is formed by two input FBGs for the wavelengths 1.273 and 1.533 μm and three output FBGs for the wavelengths 1.089, 1.273, and 1.533 μm. All the FBGs, except that for the second 1.533-μm Stokes component at the resonator output, have the reflectivity 100 %.

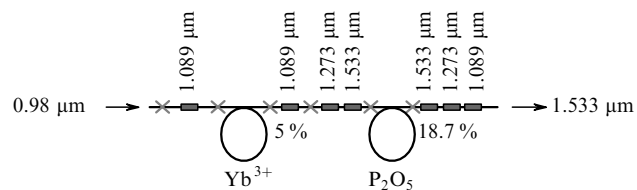


Figure 1. Scheme of the Raman fibre converter (0.98 μm is the radiation wavelength of the diode array).

The powers of the pump radiation and two Stokes components in the stationary state are described by a system of ordinary differential equations [7, 8]

$$\begin{aligned} \frac{dP_p^\pm}{dz} &= \mp\alpha_p P_p^\pm \mp \frac{\lambda_{S1}}{\lambda_p} g_1 (P_{S1}^+ + P_{S1}^-) P_p^\pm, \\ \frac{dP_{S1}^\pm}{dz} &= \mp\alpha_{S1} P_{S1}^\pm \mp \frac{\lambda_{S2}}{\lambda_{S1}} g_2 (P_{S2}^+ + P_{S2}^-) P_{S1}^\pm \\ &\quad \pm g_1 (P_p^+ + P_p^-) P_{S1}^\pm, \\ \frac{dP_{S2}^\pm}{dz} &= \mp\alpha_{S2} P_{S2}^\pm \pm g_2 (P_{S1}^+ + P_{S1}^-) P_{S2}^\pm \end{aligned} \quad (1)$$

O.N. Egorova, A.S. Kurkov, O.I. Medvedkov, V.M. Paramonov,
E.M. Dianov Fiber Optics Research Center, A.M. Prokhorov General
Physics Institute, Russian Academy of Sciences, ul. Vavilova 38, 119991
Moscow, Russia; e-mail: egorova@fo.gpi.ru

Received 12 January 2004; revision received 9 November 2004

Kvantovaya Elektronika 35 (4) 335–338 (2005)

Translated by M.N. Sapozhnikov

with the boundary conditions describing reflection from FBGs and pump radiation coupling into the resonator:

$$\begin{aligned} P_p^+(0) &= P_{\text{in}}, & P_p^-(L) &= R_p P_p^+(L), \\ P_{S1}^+(0) &= R_{S1} P_{S1}^-(0), & P_{S1}^-(L) &= R_{S1} P_{S1}^+(L), \\ P_{S2}^+(0) &= R_{S2} P_{S2}^-(0), & P_{S2}^-(L) &= R_{\text{out}} P_{S2}^+(L). \end{aligned} \quad (2)$$

Here, P_p , P_{S1} , and P_{S2} are powers of the pump, first, and second Stokes components propagating in the forward (+) and backward (−) directions, respectively; g_1 is the fibre gain at a wavelength of 1.273 μm upon pumping at 1.089 μm (1.089/1.273 μm); g_2 is the fibre gain at 1.533 μm upon pumping at 1.273 μm (1.273/1.533 μm); α_p , α_{S1} , α_{S2} are optical losses at the pump wavelength λ_p and at the wavelengths of the first (λ_{S1}) and second (λ_{S2}) Stokes components; z is the coordinate along the fibre axis; P_{in} is the input pump power; R_{S1} and R_{S2} are the reflectivities of FBGs for the first and second Stokes components at the input and output of the resonator; R_p and R_{out} are the reflectivities of FBGs for the pump radiation and at the resonator output; and L is the fibre length.

3. Experimental

The Raman fibre converter was pumped by a 1.089-μm double-clad ytterbium-doped fibre laser (Fig. 1). The active element of the converter was a P_2O_5 -doped fibre with the maximum difference between the refractive indices of a core and a cladding equal to 0.01 and the 1.05-μm cut-off wavelength for the first mode. Optical losses in the fibre and gains at different wavelengths are presented in Table 1.

Table 1. Optical losses and gains of the fibre under study.

Wavelength/μm	Optical losses/dB km ⁻¹	Gain/dB W ⁻¹ km ⁻¹
1.089	1.38	6.47*
1.273	0.90	5.08**
1.533	0.99	—

Notes: *The gain g_1 at a wavelength of 1.273 μm for $\lambda_p = 1.089$ μm;
** The gain g_2 at a wavelength of 1.533 μm for $\lambda_{S1} = 1.273$ μm.

Optical losses in each splicing and in the FBG were 0.1 dB on average, and the fibre length was 400 m. The reflectivity of the output FBG measured from the reflection spectrum was 18.7 %, the reflectivity of other gratings was ~ 100 %.

4. Simulation of the Raman fibre converter and comparison with experiment

The system of differential equations (1) with boundary conditions (2) was solved by the method of transfer of boundary conditions [12]. Figure 2 shows the calculated and measured radiation powers at a wavelength of 1.533 μm. One can see that the power calculated for $R_{S1} = 100$ % exceeds the measured output power of the converter.

It is obvious that the Raman converter efficiency is reduced because the reflection spectrum of the FBG is noticeably narrower than the spectral width of the intermediate Stokes component. This leads to a partial escape of

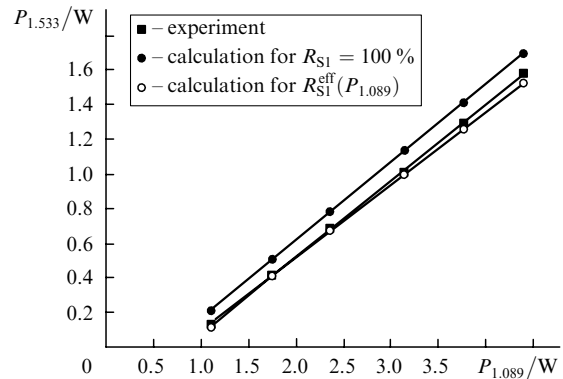


Figure 2. Experimental and calculated dependences of the radiation power at a wavelength of 1.533 μm at the output of the Raman converter on the 1.089-μm pump power for the reflectivities of the 1.273-μm FBG $R_{S1} = 100$ % and $R_{S1}^{\text{eff}}(P_{1.089})$ from Fig. 5.

the radiation power from the resonator. Figure 3 shows the spectra of the first Stokes component recorded at the resonator output for different pump powers. The hole in the spectrum is caused by reflection of radiation from the FBG. To take these losses into account, we introduced instead of the reflectivity R_{S1} in (2) the effective reflectivity for the first Stokes component, which accounts for the additional radiation power loss in the resonator.

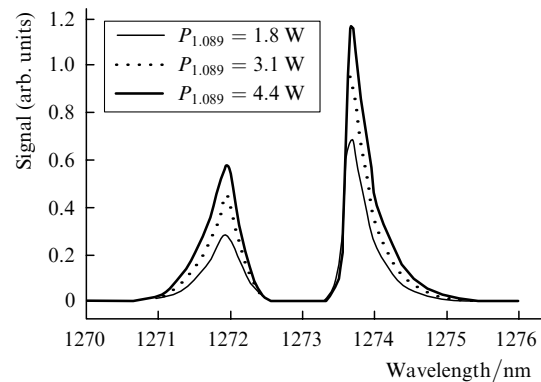


Figure 3. Emission spectra of the first Stokes component recorded at the resonator output for different 1.089-μm pump powers.

We can quite accurately determine the effective reflectivity for the first Stokes component for each value of the pump power from the power of this component calculated at the point $L = 400$ m in the resonator and the measured output power (Fig. 4). The calculated dependence of the

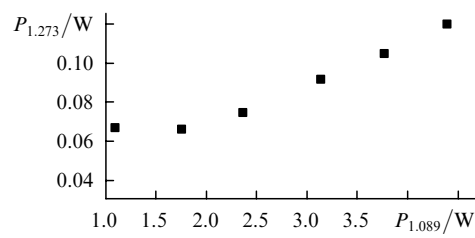


Figure 4. Dependence of the 1.273-μm output power of the resonator on the 1.089-μm pump power.

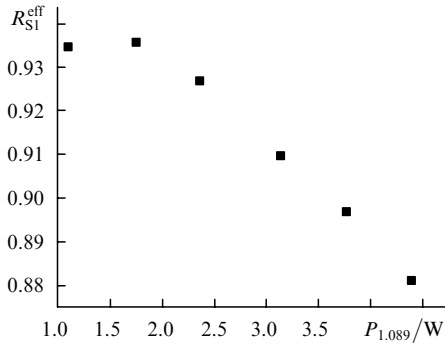


Figure 5. Calculated dependence of the effective reflectivity of the 1.273- μm FBGs on the 1.089- μm pump power.

effective reflectivity of the 1.273- μm FBG on the pump power is shown in Fig. 5. The theoretical description of the converter taking into account the effective reflectivity gives the power characteristic that is closer to the experimental one than in the case of FBGs with $R_{\text{SI}} = 100\%$ (see Fig. 2).

As the pump power is increased, the effective reflectivity decreases, which suggests the spectral broadening of the first Stokes component. We measured the spectrum of this component inside the resonator for different pump powers and found that the width of the spectrum did increase with increasing pump power (the widths of the spectra in Fig. 6b were obtained by approximating the lines by Gaussians).

The broadening mechanism of the first Stokes component is not clear at present. In our opinion, several reasons can exist. The intermediate Stokes component is broadened

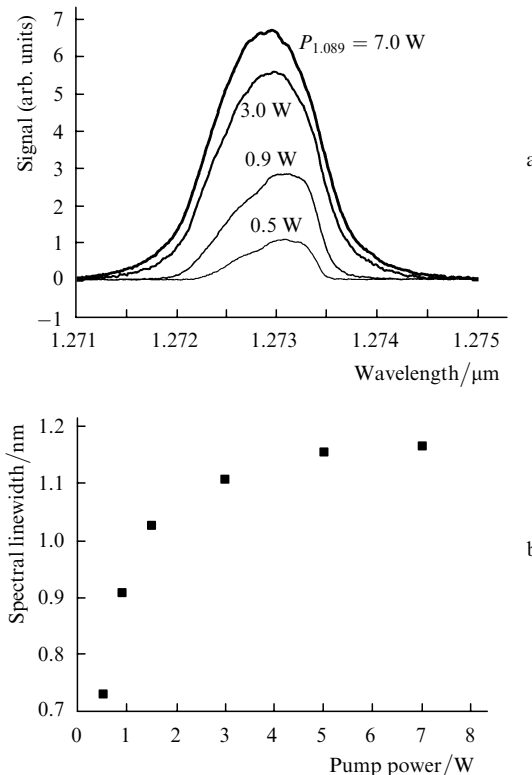


Figure 6. Emission spectra of the first Stokes component inside the Raman converter resonator for different pump powers (a) and the dependence of the width of a Gaussian approximating the emission spectra of the first Stokes component on the 1.089- μm pump power (b).

due to the filling of the spectral range (0.5–0.7 nm) of the FBG with a high reflectivity (99%). This process is more intense for high pump levels, when the next Stokes component is generated. In this case, the additional pump power efficiently transforms to this component. Under these conditions, the central component in fact ceases to grow, however, a further increase in the first Stokes component can occur at the wings of the line. The spectrum can be also broadened due to the four-wave mixing of different longitudinal modes of the Raman laser accompanied by radiation at a wavelength outside the reflection spectrum of the FBG. This radiation can be amplified by the pump radiation due to SRS.

5. Effect of the additional power losses of the first Stokes component on the optimal parameters of the two-stage Raman converter

The efficiency of a Raman converter depends on the resonator length and the reflectivity of the output FBG. For each pump power, there exist the optimal values of these parameters at which the output power of the Raman converter is maximal.

We optimised numerically the converter design. Figure 7 shows the nomograms of the dependence of the output power of the converter on the fibre length and reflectivity of the output grating. The calculation (Fig. 7a) was performed for the pump power of 4.4 W and the corresponding effective reflectivity of the 1.273- μm FBG (Fig. 5).

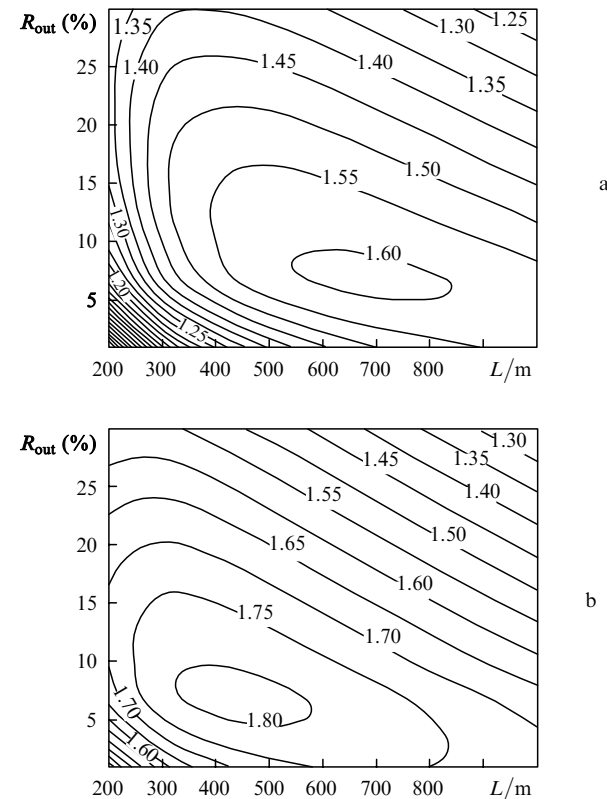


Figure 7. Calculated dependences of the output power of the converter on the fibre length and the output grating reflectivity for the real reflectivity of the 1.273- μm FBG (a) and $R_{\text{SI}} = 100\%$ (b). The pump power is 4.4 W. The numbers at the curves correspond to the calculated output power of the Raman converter in watts.

The region of the maximum output power (above 1.6 W) of the Raman converter corresponds to the fibre length $L = 600\text{--}800\text{ m}$ and the reflectivity of the output FBG $R_{\text{out}} = 5\%\text{--}10\%$. A decrease in the fibre length down to $300\text{--}400\text{ nm}$ for the value of R_{out} properly selected did not result in a significant reduction of the output power. The calculated output power of the converter with the experimental parameters $L = 400\text{ m}$ and $R_{\text{out}} = 18.7\%$ was $\sim 94\%$ of the maximum output power.

For comparison, Fig. 7b shows the dependence of the output power of the converter on L and R_{out} for the reflectivity of the $1.273\text{-}\mu\text{m}$ FBG $R_{\text{S1}} = 100\%$. In this case, the regions of optimal values of the resonator length and FBG reflectivity R_{out} are $300\text{--}600\text{ m}$ and $5\%\text{--}10\%$, respectively. Therefore, when the additional losses of the intermediate Stokes component in the resonator are taken into account, the optimal length of the resonator increases.

6. Conclusions

We have found out that the calculated output power of the Raman fibre converter ($1.089/1.273/1.553\text{ }\mu\text{m}$) in the quasi-monochromatic approximation exceeds the experimental output power. This is explained by the fact that the model ignores the additional power losses appearing because the spectral width of the first $1.273\text{-}\mu\text{m}$ Stokes component exceeds the width of the reflection spectrum of the corresponding FBG. The consideration of additional power losses of the first Stokes component caused by the mismatch between the spectral profiles provided good agreement with the experimental data.

The parameters of the Raman converter resonator were optimised for the pump power $P_p = 4.4\text{ W}$ taking into account or neglecting the additional losses of the first Stokes component. The ranges of the optimal resonator length and the output grating reflectivity for the model considering the additional losses are $600\text{--}800\text{ m}$ and $5\%\text{--}10\%$, respectively, as compared to $300\text{--}600\text{ m}$ and $5\%\text{--}10\%$ for the model neglecting these losses.

Calculations based on expressions (1) and (2) taking into account the additional losses of the intermediate Stokes component show that a proper selection of the reflectivity of the output FBG allows one to decrease considerably the resonator length only weakly reducing the output power of the Raman converter. Thus, for $L = 400\text{ m}$ and $R_{\text{out}} = 18.7\%$, the calculated output power exceeds 94% of the maximum power.

Acknowledgements. The authors thank K.G. Leont'ev for his help in the numerical solution of Eqns (1) and (2) and also I.A. Bufetov, A.V. Shubin, and M.E. Likhachev for measuring the fibre parameters.

References

1. Grubb S.G., Strasser T., Cheung W.Y., Reed W.A., Mizrahi Y., Erdogan T., Lemaire P.J., Vengsarkar A.M., DiGiovanni D.J., Peckham D.W., Rochney B.H. *Proc. Optical Amplifiers and their Applications* (Davos, Switzerland, 1995) paper SaA4-1, p. 197.
2. Dianov E.M., Grekov M.V., Bufetov I.A., Vasiliev S.A., Medvedkov O.I., Plotnichenko V.G., Koltashev V.V., Belov A.V., Bubnov M.M., Semjonov S.L., Prokhorov A.M. *Electron. Lett.*, **33** (18), 1542 (1997).
3. Dianov E.M., Grekov M.V., Bufetov I.A., Mashunsky V.M., Sazhin O.D., Prokhorov A.M., Devyatkh G.G., Guryanov A.N., Khopin V.F. *Electron. Lett.*, **34** (7), 669 (1998).
4. Kurkov A.S., Paramonov V.M., Egorova O.N., Medvedkov O.I., Dianov E.M., Zalevskii I.D., Goncharov S.E. *Kvantovaya Elektron.*, **32**, 747 (2002) [*Quantum Electron.*, **32**, 747 (2002)].
5. Zakharov S.D., Ivanov A.V. *Kvantovaya Elektron.*, **29**, 192 (1999) [*Quantum Electron.*, **29**, 1031 (1999)].
6. Yeung J.Au., Yariv A. *J. Opt. Soc. Am.*, **69** (6), 803 (1979).
7. Reed W.A., Coughram W.C., Grubb S.G. *Proc. Opt. Fiber Commun. Conf.* (San Diego, Cal., 1995) paper WD1, p. 107.
8. Rini M., Crisciani I., Degiorgio V. *IEEE J. Quantum Electron.*, **36** (10), 1117 (2000).
9. Kurukitkoson N., Sugahara H., Turitsyn S.K., Egorova O.N., Kurkov A.S., Paramonov V.M., Dianov E.M. *Electron. Lett.*, **37** (21), 1281 (2001).
10. Karpov V.I., Clements W.R., Dianov E.M., Papernyi S.B. *Can. J. Phys.*, **78**, 407 (2000).
11. Bufetov I.A., Bubnov M.M., Larionov Y.V., Medvedkov O.I., Vasiliev S.A., Melkoumov M.A., Rybaltovsky A.A., Semjonov S.L., Dianov E.M., Gur'yanov A.N., Khopin V.F., Durr F., Limberger H.G., Salathe R.-P., Zeller M. *Laser Phys.*, **13** (2), 234 (2003).
12. Moiseev N.N. *Elementy teorii optimal'nykh sistem* (Elements of the Theory of Optimal Systems) (Moscow: Nauka, 1975).